An Internal Deletion in the Cytoplasmic Tail Reverses the Apical Localization of Human NGF Receptor in Transfected MDCK Cells

Andre Le Bivic,‡ Yula Sambuy,§ Alexandra Patzak,* Nila Patil,* Moses Chao,* and Enrique Rodriguez-Boulan*

*Department of Cell Biology and Anatomy, Cornell University Medical College, New York, NY 10021; ‡Biologie de la Differenciation Cellulaire, Faculté des Sciences de Luminy, Marseille, 13288 France; and §Istituto Nazionale della Nutrizione, 00179 Rome, Italy

Abstract. A cDNA encoding the full-length 75-kD human nerve growth factor receptor was transfected into MDCK cells and its product was found to be expressed predominantly (80%) on the apical membrane, as a result of vectorial targeting from an intracellular site. Apical hNGFR bound NGF with low affinity and internalized it inefficiently (6% of surface bound NGF per hour). Several mutant hNGFRs were analyzed, after transfection in MDCK cells, for polarized surface expression, ligand binding, and endocytosis. Deletion of juxtamembrane attachment sites for a cluster of *O*-linked sugars did not alter apical localization. A mutant receptor lacking the entire cytoplasmic tail (except for the five proximal amino acids) was also expressed on the apical membrane, suggesting that information for apical sorting was contained in the ectoplasmic or transmembrane domains. However, a 58 amino acid deletion in the hNGFR tail that moved a cytoplasmic tyrosine (Tyr 308) closer to the membrane into a more charged environment resulted in a basolateral distribution of the mutant receptor and reversed vectorial (basolateral) targeting. The basolateral mutant receptor also internalized ^{125}I-NGF rapidly (90% of surface bound NGF per hour), exhibited a larger intracellular fraction and displayed a considerably shortened half-life (~3 h). We suggest that hNGFR with the internal cytoplasmic deletion expresses a basolateral targeting signal, related to endocytic signals, that is dominant over apical targeting information in the ecto/transmembrane domains. These results apparently contradict a current model that postulates that basolateral targeting is a default mechanism.

THE plasma membrane of epithelial cells displays distinct apical and basolateral domains with different sets of proteins and lipids (9, 50, 58). To establish and maintain these polarized surface domains, epithelial cells use diverse strategies including sorting and packaging of proteins and lipids into different post-Golgi transport vesicles, targeting of these vesicles to the correct domain, and stabilization and/or accurate recycling of the proteins specific for a given domain. Using different epithelial models such as liver, intestine, and kidney cells, progress was recently made in defining the pathways followed by apical and basolateral proteins from the Golgi complex to their respective domains (2, 25, 37). Two major sorting sites were established by these studies, the *trans*-Golgi network (TGN)[1] (17, 27, 28, 31, 36, 41) and the basolateral membrane (2, 25, 35, 37). To date, all basolateral proteins studied appear to be targeted directly from an intracellular sorting site (presumably the TGN) to the basolateral membrane (7, 8, 25–28, 31). Apical proteins, on the other hand, may follow direct or indirect transcytotic pathways to the apical surface, depending on the epithelial cell type (2, 25, 35, 37).

Little is known about the molecular signals that direct proteins along their respective pathways. Chimeric protein experiments designed to identify sorting domains in viral envelope glycoproteins initially localized apical and basolateral targeting information to their large, complexly folded ectodomain (12, 39, 40, 51, 54, 60). Recent studies using poly-Ig receptor (PIgR) (5), natural isoforms of the FcRII (20) and hybrids between placental alkaline phosphatase (PLAP) and VSV G protein (6) have uncovered basolateral sorting information in the cytoplasmic and/or transmembrane domains. Furthermore, anchoring to the bilayer via glycosylphosphatidylinositol (GPI) strongly correlates with apical localization (33, 34, 68) and addition of GPI to unsorted secretory proteins or to basolateral proteins resulted in their targeting to the apical surface (6, 30), indicating that interactions with the lipid bilayer are important in epithelial sorting (32, 64). Co-clustering of glycosphingolipids and apical glycoproteins in the TGN has been suggested as a factor in apical targeting

1. *Abbreviations used in this paper*: GPI, glycosyl-phosphatidylinositol; hNGFR, human nerve growth factor; PIgR, poly-IG receptor; PLAP, placental alkaline phosphatase; S-NHS-biotin, sulfo-*N*-hydroxyl-succinimido-biotin; TGN, *trans*-Golgi network; WT, wild type.

(65). All of the above suggests that signals with opposite or redundant information exist in different topological domains of a given protein but the nature of these signals, the mechanisms that decode them and the sequence of their operation remain elusive.

With the exception of the PIgR all other recombinant DNA studies searching for sorting signals in epithelial transmembrane proteins were carried out with viral envelope glycoproteins. These glycoproteins are not naturally designed to be permanently expressed in cells but to be incorporated into budding virions (60) and their tri- or tetrameric nature complicates the interpretation of fusion protein studies (52). These factors may account for some contradictions observed in studies on features that control their migration along the secretory pathway (52) and their polarized epithelial distribution (9).

In this report, we analyzed the sorting and trafficking in MDCK cells of the 75-kD human nerve growth factor receptor (hNGFR). This receptor has an NH_2-terminal ectodomain rich in cysteine residues, one *N*- and several *O*-glycosylation sites, a single transmembrane domain and a 155 amino acid cytoplasmic tail (21). When transfected into fibroblasts, it binds NGF with characteristic low affinity ($K_d \sim 10^{-9}$ M) (3). We compared its sorting and trafficking patterns with those of mutant hNGFRs with deletions of the attachment site for juxtamembrane *O*-linked oligosaccharides (which might cluster with apically targeted glycolipids), with a deletion of 150 amino acids of the cytoplasmic domain and, finally, with an internal deletion of the cytoplasmic tail. We found that the wild type receptor was targeted efficiently to the apical surface, where it bound and endocytosed poorly NGF. Deletion of *O*-linked carbohydrates or of practically the entire cytoplasmic domain did not affect its apical distribution. However, hNGFR with the internal cytoplasmic deletion displayed a strikingly modified phenotype, with a basolateral localization due to reversed targeting from the TGN, a shortened half-life and an increased endocytic ability. Our results are compatible with a transmembrane or ectodomain apical signal in the hNGFR, which behaves recessively when a basolateral signal is added to the cytoplasmic domain. Together, these data suggest that the apical and the basolateral sorting machineries recognize different topological domains of the hNGFR.

Materials and Methods

Reagents

Cell culture reagents were purchased from Gibco Laboratories (Grand Island, NY). Affinity purified antibodies (rabbit anti-mouse IgG) were purchased from Cappel Laboratories (Westchester, PA), protein A-Sepharose was from Pharmacia Fine Chemicals (Uppsala, Sweden). Sulfo-*N*-hydroxylsuccinimido-biotin (S-NHS-biotin) was from Pierce Chemical Co. (Rockford, IL). Enzymes for oligosaccharide digestions were from Boehringer-Mannheim Biochemical, Mannheim, Germany. All other reagents were obtained from Sigma Chemical Co. (St. Louis, MO).

Cells, Antibodies, and Cell Culture

MDCK cells were grown in DME supplemented with 7% FCS, penicillin (50 U/ml) and streptomycin (50 μg/ml). When grown on filters, 2×10^6 cells were seeded on Transwell chambers (24.5-mm-diam, Costar, Cambridge, MA) and cultured for at least 5 d with changes of medium ever other day. Rabbit polyclonal antibodies against gp114 were obtained as described (28). mAb (ME 20.4) against the human NGF receptor (53) was produced as ascites and used as described in the text.

Constructs

Full-length NGF receptor cDNA (WT), PS mutant, and Xba (XI) mutant were obtained as described (19) and inserted in the retroviral expression vector pMV7. Briefly, the full-length 75-kD human NGF receptor cDNA was subcloned into pBR322, digested with SacI, and religated, resulting in a receptor cDNA with an intact coding region and polyadenylation signal, but lacking 1,759 bp of the 3' untranslated region (pSL). For the mutant PS, pSL was partially digested with PvuII and StuI, religated, and a plasmid lacking the PvuII (940 nt)-StuI (1,111 nt) fragment was isolated. Following EcoRI digestion, the 1.7-kb PS receptor cDNA was subcloned into the EcoRI site of the expression vector pMV7. The XI mutant was obtained by linearization of pSL at 940 nt with partial PvuII digestion. Universal termination Xba linkers (Biolabs, Beverly, MA) were ligated to the linearized plasmid, cut with XbaI, and religated to generate a TAG termination codon at the PvuII site. The 2.0-kb fragment containing the receptor cDNA was subcloned into the EcoRI site of pMV7. The BSTE (BE) mutant was generated by BSTEII digestion of pSL at position 805 and 838 and inserted in the vector pMV7.

Transfection and Clonal Selection

MDCK type II cells were transfected using the DNA-calcium phosphate procedure as described (15) and clones expressing the neomycin-resistance marker selected in G418 (0.5 mg/ml) medium. G418-resistant colonies were screened for expression of the NGFR by a rosetting assay involving sequential exposure to the ME 20.4 antibody and to red blood cells coated with rabbit anti-mouse antibodies (14). Positive colonies were isolated with cloning cylinders, cloned again by limited dilution, and screened for hNGFR expression by ELISA and immunofluorescence.

Immunofluorescence and Frozen Sections

Procedures for indirect immunofluorescence of transfected MDCK cells were as described (49). For intracellular staining, fixed cells were permeabilized with 0.075% saponin. Rhodamine-conjugated goat anti-mouse antibodies (Jackson, West Grove, PA) were used at 1/100. Semi-thin frozen sections were performed by a modification (66) of a procedure by Tokuyasu (62). Ultra-thin frozen sections were prepared according to Griffiths et al. (18). Immunocytochemistry was performed by washing with PBS containing 10% FCS and staining with the ME 20.4 antibody followed by rabbit anti-mouse IgG and protein A-5-nm colloidal gold at pH 8 (59). Sections were contrasted as previously described (59).

Cell Surface Biotinylation

Biotinylation of confluent monolayers on Transwells with s-NHS-biotin was carried out three times for 20 min as described (56). After immunoprecipitation, samples were analyzed by SDS-PAGE and transferred to nitrocellulose. Biotinylated proteins were then revealed by blotting with ^{125}I-streptavidin (56).

Pulse-Chase Experiments and Cell Surface Immunoprecipitation

Cells grown on filters were incubated for 30 min in DME without cysteine and pulsed for 20 min in the same medium containing 1 mCi/ml of ^{35}[S]cysteine (New England Nuclear, Boston, MA) as described (27). After a wash with DME, the cells were chased in DME containing 5× the normal cysteine concentration. For cell surface immunoprecipitation, antibodies were added to the chase medium (10 μl of ascites/ml) for 2 h at 4°C or 3 h at 37°C. After incubation the filters were washed five times, 10 min each, with DME containing 0.5% BSA, and lysed as described (27). The binding of ME 20.4 antibodies to hNGFR was assayed by ELISA in a pH range from 5 to 7.5 and found to be pH independent.

Immunoprecipitation and Glycosidase Digestions

Lysates of labeled cells were immunoprecipitated as described (27) using the mAb ME 20.4 (5 μl/ml) preabsorbed on Protein A-Sepharose beads coupled to rabbit anti-mouse antibodies. Immunoprecipitates were digested with neuraminidase (50 mU/sample) and *O*-Glycanase (4 mU/sample) after

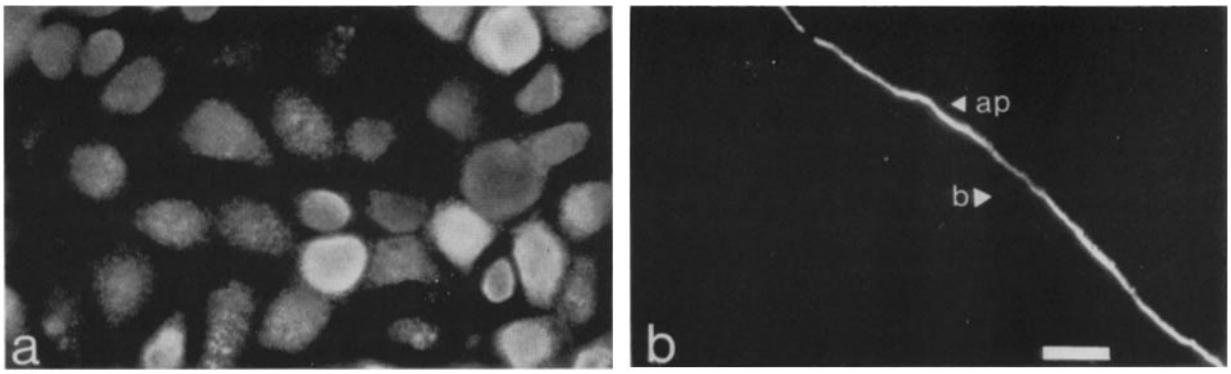

Figure 1. Apical localization of WT hNGFR expressed in MDCK cells. MDCK cells transfected with hNGFR cDNA were grown at confluency and hNGFR was detected by indirect immunofluorescence using monoclonal antibody ME 20.4 either en face (*a*) or on semithin frozen sections (*b*). *ap*, apical side; *b*, basal side. The labeling is predominantly associated to the apical surface of the cells. Bar, 5 μm.

release from the beads by boiling in 50 mM sodium acetate containing 0.1% SDS. Before digestion, Triton X-100 (to a final concentration of 1%) and protease inhibitors were added as described (61).

NGF Binding and Internalization Studies

NGF was radioactively labeled with Na^{125}I using the chloramine T procedure (16) at a specific activity of 2.5 μCi/pmole. Cells on filters were incubated with 300 μl of DME containing 1 ng/ml of ^{125}I-NGF (either apically or basolaterally) and DME on the other side. After incubation the cells were washed three times with PBS Ca/Mg at 4°C. Surface bound and internalized ^{125}I-NGF (3) fractions were determined by incubating the cells with 1 ml of ice-cold 0.2 M acetic acid containing 0.5 M NaCl for 5 min on ice. An additional wash was performed with the same buffer and the two washes were pooled. The filters were then excised and the samples were counted in a gamma-counter (Beckman Instruments, Inc., Palo Alto, CA). Non-specific binding was determined by adding a 1,000-fold excess of cold NGF to the radioactive NGF. Acid-released radioactivity was considered to be surface bound whereas acid-resistant radioactivity was a measure of internalized ligand (3).

Results

Polarized Expression of hNGFR in Transfected MDCK Cells

A cDNA encoding the 75-kD human NGF receptor was expressed in type II MDCK cells using the retroviral expression vector pmVE1. After selection with the neomycin analog G418, resistant cells were screened for expression with a rosetting assay. Positive cells were cloned twice by limiting dilution and clones expressing hNGFR identified by indirect immunofluorescence using a mAb, ME 20.4. Two independent clones were studied with identical results.

A strong labeling of the apical domain was observed by indirect immunofluorescence on paraformaldehyde-fixed monolayers en face (Fig. 1 *a*) and on semithin frozen sections (Fig. 1 *b*). A much lower expression was detected on the basolateral membrane. The apical localization was confirmed at the ultrastructural level by indirect gold labeling on ultrathin frozen sections (Fig. 2). An intense labeling was observed on apical microvilli and on intermicrovillar areas while much lower gold levels were observed on the basal and lateral membranes. To quantify the polarity of the hNGFR we used a biotin assay (56). MDCK monolayers grown on filters were labeled with S-NHS-biotin from the apical or from the basolateral side. Biotinylated hNGFR was revealed by immunoprecipitation, SDS-PAGE and ^{125}I-streptavidin blotting (Fig. 3). We found that 80% of the receptor was apical; a control apical marker, Gp114 (28, 55), the major apical sialoglycoprotein of MDCK cells, was somewhat better polarized, >90% apical, in the same cells.

Expression of hNGFR Mutants in MDCK Cells

Having established that the wild type hNGFR (WT hNGFR) is sorted apically, we carried out experiments to determine the localization of the sorting information in this protein. We expressed in MDCK cells three constructs containing different deletions (Fig. 4 *A*) to test different hypotheses on possible targeting signals. The BE mutant receptor has a deletion of several potential juxtamembrane attachment sites for a cluster of *O*-linked carbohydrate side chains which, because of their position near the bilayer, might interact with glycolipid carbohydrates in the bilayer and mediate apical sorting. The XI mutant hNGFR has a deletion of the entire cytoplasmic domain with the exception of the five amino acids closest to the membrane; this construct was used to test the contribution of the cytoplasmic tail to apical sorting. Finally, the PS mutant receptor has a deletion in the cytoplasmic domain that places Tyr308, normally 64 amino acids away from the membrane, in a position closer to the bilayer. In this position (seven amino acids away from the last hydrophobic amino acid) the tyrosine residue is surrounded by several charged aminoacids (Ser, Lys, Arg, and Asn) resembling the environment recently described by Ktistakis et al. (23) as being most favorable to induce endocytosis of the normally poorly internalized influenza HA (Fig. 4 *B*). The second cytoplasmic tyrosine (Tyr340) is surrounded by hydrophobic amino acids (Fig. 4 *B*) and is thus not expected to play an important role in endocytosis.

These constructs were transfected in MDCK cells and stable clones expressing hNGFR, as assayed by indirect immunofluorescence, were obtained. To estimate the level of mutant hNGFR expression in the selected clones, as compared to WT hNGFR, cells were pulsed with ^{35}[S]cysteine for 3 h and the different hNGFR mutants were immunoprecipitated and analyzed by SDS-PAGE and fluorography (Fig. 5 *A*). WT hNGFR had the strongest level of expression and the XI mutant the weakest. The apparent molecular weights of the protein products were in good agreement with the sizes

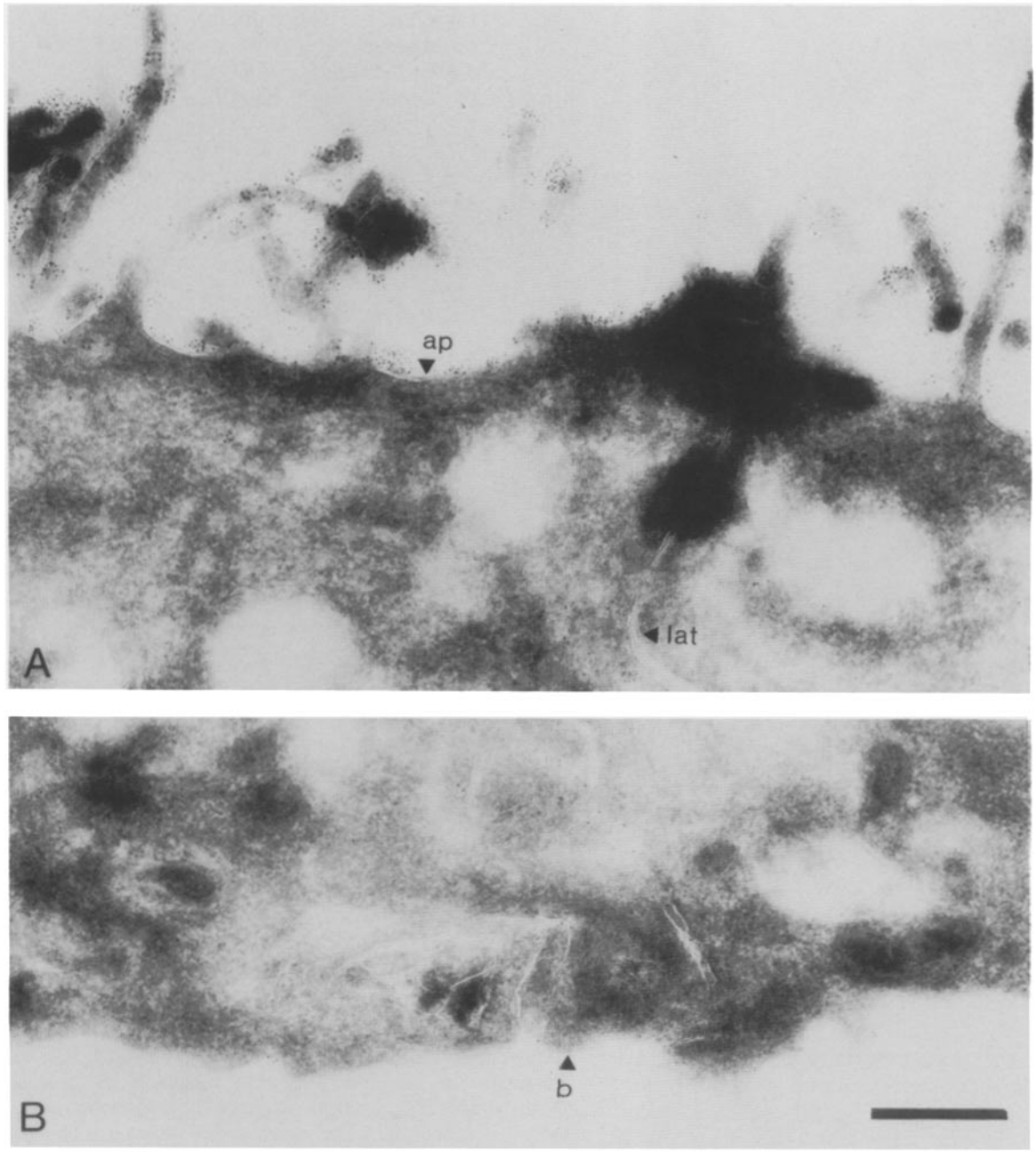

Figure 2. Ultrastructural localization of WT hNGFR. Ultrathin frozen sections of confluent MDCK cells expressing hNGFR were stained with ME 20.4, affinity purified rabbit anti-mouse IgG and 5-nm gold protein A. Most of the gold particles accumulate on the apical membrane and some can be seen on the basolateral membrane. *ap*, apical membrane; *lat*, lateral membrane; *b*, basal membrane. Bar, 0.3 μm.

of the deletions introduced. To determine whether the mutants were correctly processed, we followed the acquisition of complex carbohydrate chains by a 20-min metabolic pulse with ^{35}[S]cysteine, followed by a chase (Fig. 5 *B*). A shift in the apparent molecular weight was observed for all the mutants during the chase; processing occurred with identical half-times (~30 min) indicating that the mutations introduced did not affect folding, exit from the ER, or migration along the secretory pathway (52). The WT, BE, and XI mutants were stable over 6 h while the PS mutant was rapidly degraded with a half-life of ~3 h. The addition of *O*-linked sugars was monitored by Neuraminidase and *O*-Glycanase treatment of hNGFR immunoprecipitated from cells labeled for 16 h with ^{35}[S]cysteine. The WT, XI, and PS mutant proteins showed a shift in their migration on SDS-PAGE after digestion by both Neuraminidase and *O*-Glycanase but a shift in the electrophoretic mobility of the BE mutant protein was not detected, consistent with a deletion of its *O*-glycosylation sites (data not shown).

Polarized Expression of the hNGFR Mutants in MDCK Cells

We investigated the cellular distribution of the hNGFR mutants expressed in MDCK cells. Indirect immunofluorescence on fixed intact cells detected a clear punctate apical

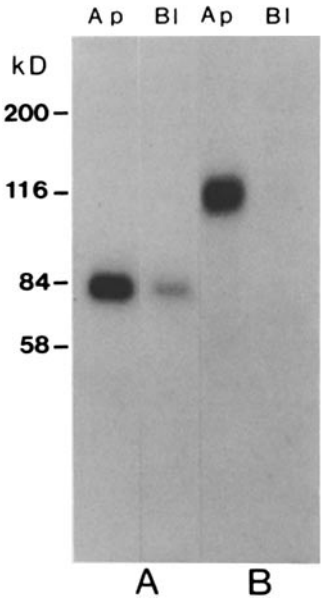

Figure 3. Polarity of surface WT hNGFR expressed in MDCK cells. MDCK cells expressing the hNGFR were grown on filters and biotinylated either from the apical (*Ap*) or the basolateral (*Bl*) side. After immunoprecipitation the hNGFR (*A*) or the endogenous apical protein Gp114 (*B*) were detected by ^{125}I-streptavidin blotting. hNGFR is predominantly labeled from the apical side (80%) as is Gp114 (90%).

staining in WT, BE, and XI hNGFR expressing cells (Fig. 6, *A–C*), while no staining could be seen in PS hNGFR and untransfected MDCK cells (Fig. 6, *D* and *E*). When the cells were permeabilized with saponin, PS hNGFR expressing cells showed specific fluorescence on the basolateral membrane and on perinuclear vesicles (Fig. 6 *I*).

To confirm these localizations we used surface immunoprecipitation (25) since labeling with S-NHS-biotin gave signals too weak to be quantified in the case of the XI and the PS hNGFR mutants (not shown). Cells expressing the WT, BE, XI, and PS mutants of hNGFR were grown on filters for 6 d and were labeled overnight with ^{35}[S]cysteine. The cells were then incubated for 2 h with ME 20.4 antibodies added to the apical or the basolateral medium at 4°C. After several washes at 4°C the cells were lysed, the WT, and mutant hNGFR-antibody complexes precipitated with Protein A-Sepharose beads and analyzed by SDS-PAGE followed by fluorography (Fig. 7). WT, BE, and XI hNGFRs were predominantly (>80%) precipitated by apical antibody. On the other hand, <5% of surface PS hNGFR could be precipi-

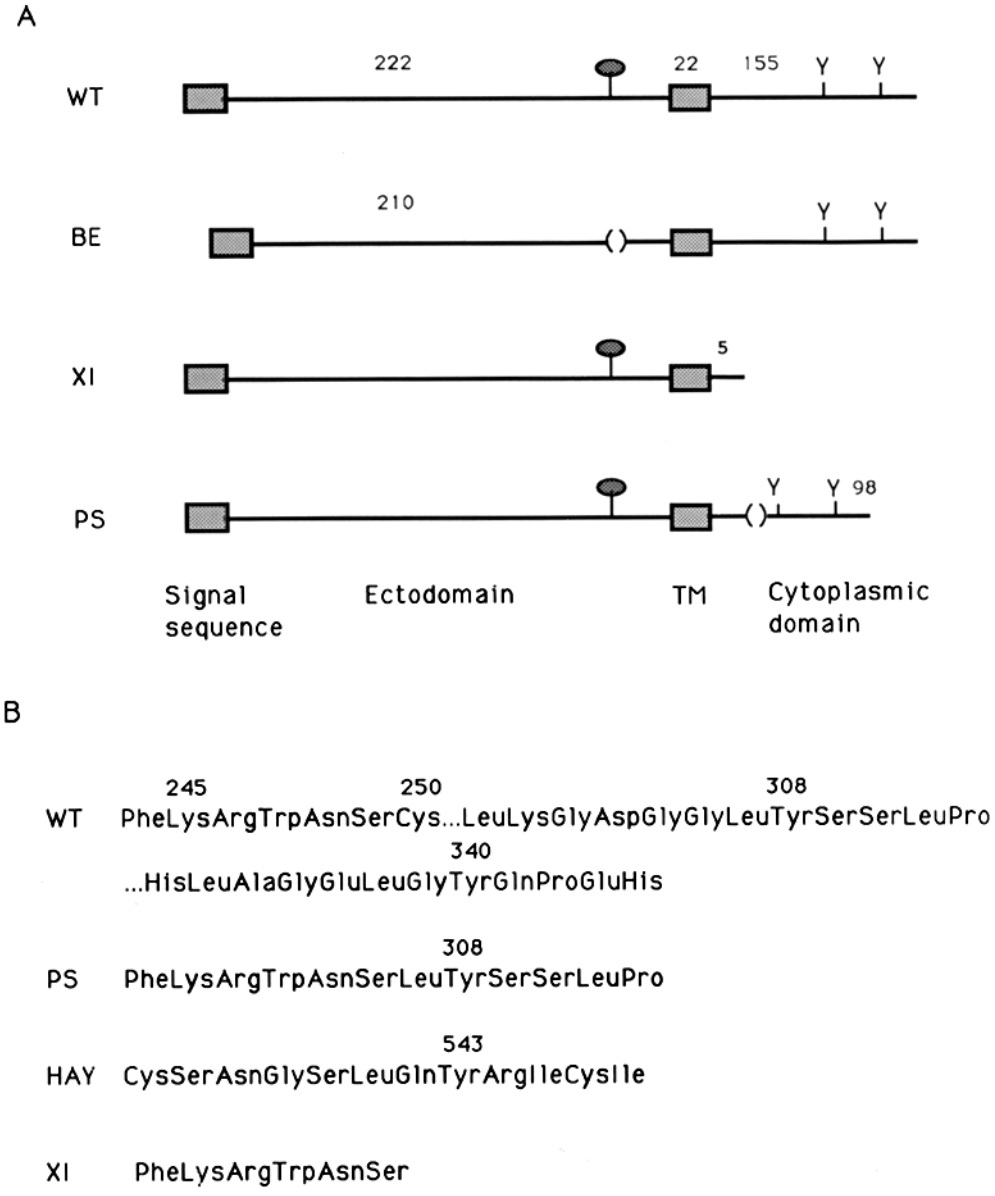

Figure 4. Scheme of hNGFR cDNA mutants. (*A*) The boxes and lines represent the signal sequence, the cysteine-rich ectodomain, the transmembrane (*TM*) domain, and the cytoplasmic domain of the hNGFR. All cDNAs contain the native hNGFR polyadenylation site. *WT*, full-length cDNA; *BE*, deletion from amino acid 203 to amino acid 215. (*XI*) Deletion of the last 150 aa residues on the COOH-terminal side. (*PS*) Deletion from amino acid 276 to amino acid 333. The number of amino-acids residues per domain are given and the sign in the ectodomain close to the transmembrane domain represents a cluster of O-linked sugars. (*Y*) Tyrosine residues in the cytoplasmic domain. (*B*) The sequences around tyr308 are shown for WT hNGFR and for PS hNGFR. The sequence surrounding tyr543 in the endocytic mutant of influenza HA (23) and the cytoplasmic tail of the XI mutant of hNGFR are also shown.

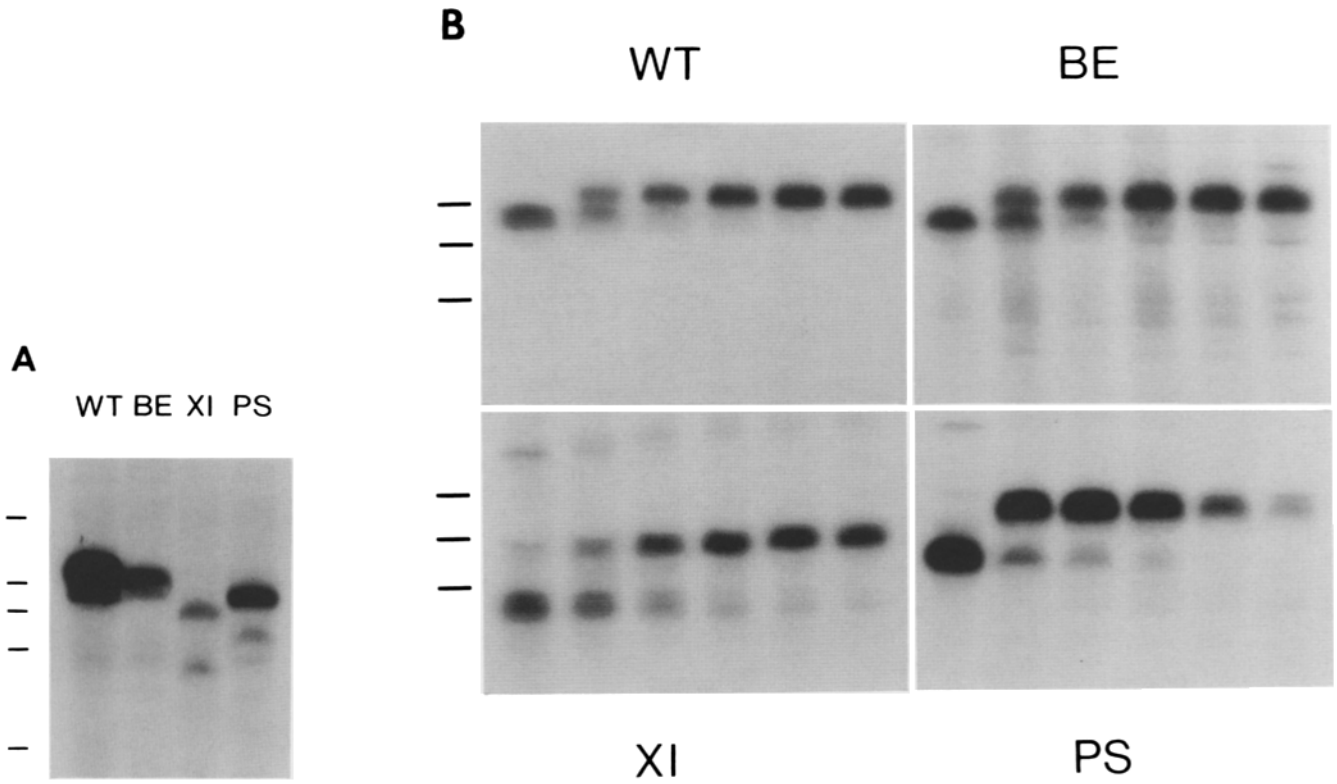

Figure 5. Expression and processing of the hNGFR mutants in MDCK cells. (*A*) Clones of MDCK cells expressing the different hNGFR mutants were labeled 3 h with 0.25 mCi/ml of ^{35}[S]cysteine and the hNGFR mutants were immunoprecipitated and analyzed by SDS-PAGE and fluorography. Bars on the left indicate the migration of molecular weight standards, from top to bottom: 180, 116, 84, 58, and 45 kD. (*B*) Clones of MDCK cells expressing the different hNGFR mutants were pulsed for 20 min with 1 mCi/ml of ^{35}[S]cysteine and chased for 0, 30, 60, 120, 240, and 360 min with cold cysteine. After immunoprecipitation, the hNGFR mutants were analyzed by SDS-PAGE gel and fluorography. Exposure times were 1 h for the WT, 10 h for the BE and the PS and 20 h for the X1 mutant. Bars on the left represent (from top to bottom) the 84, 58, and 45 kD molecular weight standards.

tated from the apical side; most of the surface fraction was basolateral (>95%), confirming the reversed polarity of this mutant receptor. Furthermore, PS hNGFR displayed the largest fraction of intracellular (surface antibody inaccessible) molecules (not shown). As a control, the polarity of Gp114 was assayed by the biotin polarity assay in the same cells and found to be apical (~90%) in all clones (data not shown) indicating that the reversed polarity of PS hNGFR was not the result of a generalized reversion of all apical proteins.

The reversed polarity of PS hNGFR may have two possible explanations. Either the receptor is targeted directly to the apical surface and is then transcytosed, or the mutation results in its reversed targeting from the Golgi apparatus to the basolateral surface. To distinguish between these two possibilities, we compared the targeting of newly synthesized hNGFR in the WT and the PS mutants using a continuous antibody targeting assay that we previously described (25). Confluent monolayers grown on filters were pulsed for 20 min and then chased for 180 min at 37°C in the presence of hNGFR antibodies added either to the apical or to the basolateral media. After several washes at 4°C the cell extracts were immunoprecipitated and analyzed by SDS-PAGE and fluorography. Less than 20% of newly synthesized WT hNGFR could be detected by continuously added basolateral antibodies, whereas >80% was bound by apical antibodies indicating that the apical pool of WT hNGFR reached directly the apical surface from the Golgi apparatus (Fig. 8, *WT*). On the other hand, >90% of newly synthesized surface PS hNGFR bound to basolateral antibodies and almost none to apical antibodies continuously added during the time of surface delivery, which is consistent with reversed (basolateral) targeting (i.e., opposite to WT hNGFR) (Fig. 8, *PS*). PS hNGFR displayed a larger (antibody inaccessible) intracellular fraction than WT hNGFR.

Binding and Internalization of ^{125}I-NGF

Cells expressing PS hNGFR showed strong specific intracellular immunofluorescence (Fig. 6), a large intracellular fraction inaccessible to surface immunoprecipitation (Fig. 8) and a normal Golgi processing coupled with a rapid degradation rate (Fig. 5 *B*). All of these parameters are consistent with increased internalization. To directly compare its endocytic capacity with that of WT and other mutant hNGFRs, we measured the binding and internalization of ^{125}I-NGF from the apical and from the basolateral sides of filter-grown monolayers. Binding assays were performed at 37°C. Scatchard analysis of binding to WT hNGFR indicated a single binding constant (K_d = 7.5 × 10^{-10} M, comparable to that of low affinity NGF receptors (3) (data not shown). The affinity for NGF is not expected to be changed by any of the

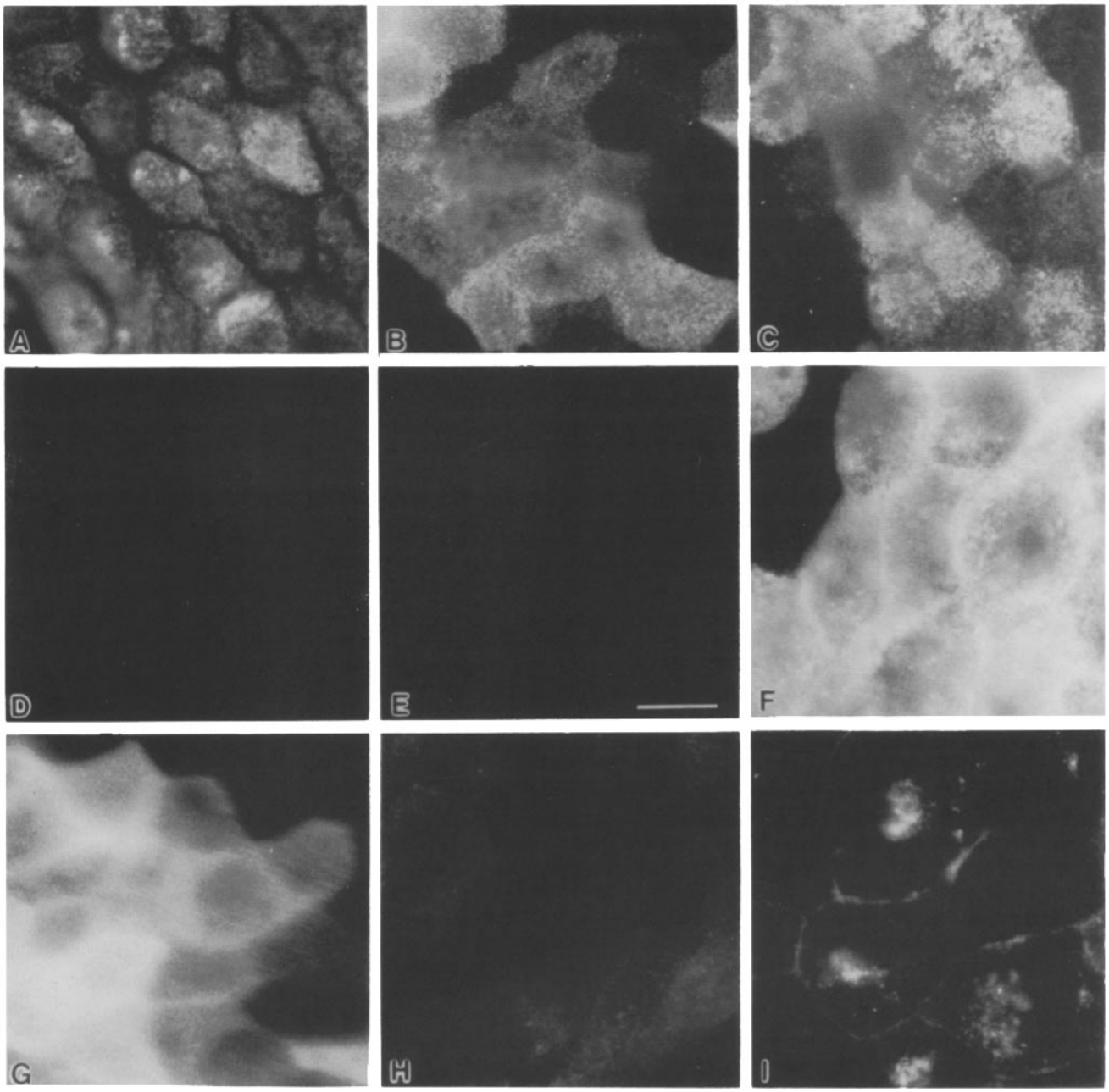

Figure 6. Indirect immunofluorescence localization of the hNGFR mutants expressed in nonpermeabilized and permeabilized MDCK cells. Cells were grown on coverslips and fixed with 2% paraformaldehyde 3 d after confluency. The cells were then incubated in the absence (*A* to *E*) or the presence of 0.075% saponin (*F* to *I*) with the ME 20.4 antibody followed by a FITC-goat anti-mouse antibody. Surface labeled cells (*A* to *E*) were photographed at the plane of the apical membrane while pictures of permeabilized cells (*F* to *I*) were taken below the plane of the apical membrane. (*A* and *F*) WT hNGFR mutant. (*B* and *G*) BE hNGFR mutant. (*C* and *H*) X1 hNGFR mutant. (*D* and *I*) PS hNGFR mutant. (*E*) Nontransfected MDCK cells. Bar, 10 μm.

mutations studied here since the binding site resides in the fourth cysteine repeat of the ectodomain (Yan, H., and M. Chao, manuscript in preparation), a region not affected by these mutations. A similar low affinity binding is observed in fibroblasts and melanoma cells transfected with 75-kD hNGFR (21, 46). Surface and internalized (apical or basolateral) fractions of the ligand were determined as acid sensitive and acid-resistant ^{125}I-NGF (see Materials and Methods). In spite of a 100–200-fold reduction in surface expression and 10–14-fold reduction in total expression, PS hNGFR transfected MDCK cells accumulated in 1 h at 37°C 30% more ^{125}I-NGF than WT hNGFR transfected cells (Fig. 9), thus showing a high endocytic capacity. Of the total cell-associated ^{125}I-NGF, 93% was acid insensitive (intracellular) in PS hNGFR cells after 1-h binding, whereas the opposite (94% at the cell surface) was observed for WT hNGFR in the same time. The BE and X1 hNGFR mutants showed three- and fivefold increases in ^{125}I-NGF internalization with regard to WT.

Interestingly, wild type and mutant receptors internalized

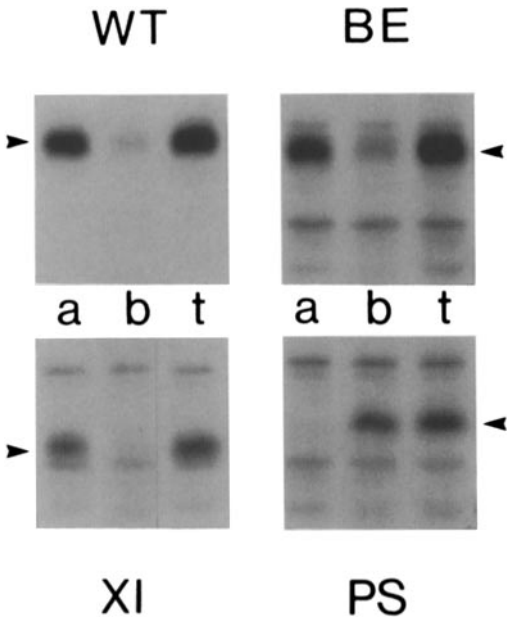

Figure 7. Surface immunoprecipitation of hNGFR mutants expressed in MDCK cells. Cells grown on filters for 6 d were labeled overnight with 0.2 mCi/ml of ^{35}[S]cysteine. After a 1-h chase, the cells were incubated at 4°C with ME 20.4 antibodies (10 μl/ml) either in the apical (*a*) or in the basolateral (*b*) medium, or in both (+) for 2 h. The cells were then washed extensively and the hNGFR-ME 20.4 complexes were precipitated with protein A-Sepharose beads. The immunoprecipitates were analyzed by SDS-PAGE and fluorography. WT hNGFR and the BE and XI mutants were precipitated predominantly from the apical side while the PS mutant was mainly precipitated from the basolateral side. Arrowheads denote the hNGFR mutants; the other bands seen are non specific products from the immunoprecipitation, as they are observed in all lanes.

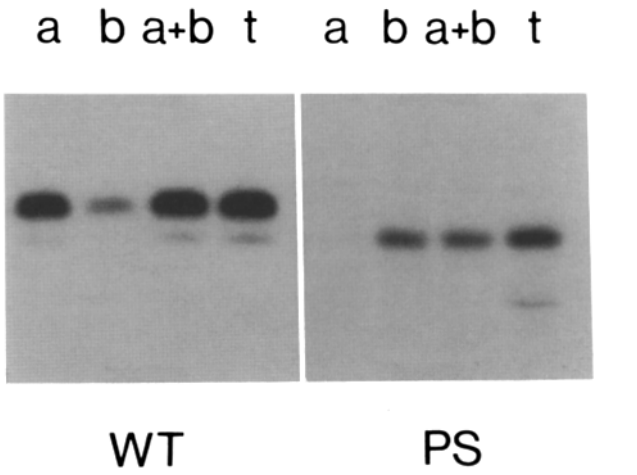

Figure 8. Targeting of WT and PS hNGFR mutants expressed in MDCK cells. Cells grown on filters were pulsed for 20 min with ^{35}[S]cysteine (1 mCi/ml) then chased for 180 min in the absence (*t*) or in the presence of ME 20.4 antibodies (10 μl/ml) added to apical (*a*), basolateral (*b*), or both sides (*a*+*b*). Cells were then washed thoroughly and ME 20.4-hNGFR complexes were extracted and precipitated with protein A-Sepharose beads. A sample was directly immunoprecipitated with ME 20.4 antibodies (*t*). After SDS-PAGE, hNGFR, and its mutants were detected by fluorography. WT hNGFR was mainly detected on the apical side while PS hNGFR was detected on the basolateral side, indicating an opposite intracellular sorting of the two hNGFR forms.

NGF more efficiently from the basolateral than from the apical side; this internalization was specific since it was not observed in untransfected MDCK cells under the same experimental conditions (Fig. 9). WT, BE, and XI internalized approximately three to four times more NGF from the basal than from the apical side, in site of a fourfold apical concentration. PS hNGFR internalized ~30 times more NGF from the basal than from the apical side, consistent with its concentration on the basal surface. Furthermore, the coefficient surface/internalized (basolateral) ^{125}I-NGF was much lower than one for PS hNGF, but always greater than one for WT, BE, and XI NGFR, indicating that the 57 cytoplasmic amino acid deletion introduced into PS hNGFR largely increased its ability to endocytose its ligand. Thus, the increased endocytosis of PS hNGFR depends on both an intrinsic change in its structure and on its basolateral localization, which promotes the endocytosis of all hNGFR constructs.

Discussion

We have used hNGFR as a model to study the signals that direct polarized protein targeting in epithelial cells. In MDCK cells transfected with a full-length cDNA coding for WT hNGFR, the receptor was *N*- and *O*-glycosylated, migrated to the Golgi apparatus within 20–30 min and was transported to the cell surface with a half-time of ~40 min. In confluent monolayers, WT hNGFR was apically polarized, as shown by indirect immunofluorescence en face and on semi-thin frozen sections, by immuno-gold labeling on ultra-thin frozen sections, by a biotin polarity assay, by cell surface immunoprecipitation and by ^{125}I-NGF binding to filter-grown cells. Quantitatively, 80% of the WT hNGFR was present on the apical side; this polarity was somewhat lower than observed for a major apical sialoglycoprotein of MDCK cells, Gp114 (28, 55), which was 90% apical with the same biotin polarity assay. An antibody targeting assay that was used previously to demonstrate the transcytotic pathway of an apical glycoprotein in Caco-2 cells (25) showed that the apical distribution of hNGFR resulted from vectorial targeting from an intracellular site, presumably the TGN. Therefore, hNGFR follows the pattern of all apical proteins of MDCK cells studied to date (28, 31, 36, 41). The somewhat lower polarity of hNGFR (compared with Gp114) may have three possible explanations. First, the apical targeting machinery may recognize less efficiently apical information in hNGFR than in Gp114. Second, the receptor might be partially transcytosed after delivery to the apical surface. Third, hNGFR may have some basolateral targeting information competing with apical targeting information.

A possible role of NGFR in transcytosis is suggested by previous work that described a low efficiency uptake on NGF by the intestine of newborn rats (57); however, the presence of the receptor was not established in these studies. Interestingly, in this regard, a cell line derived from a human colon adenocarcinoma, SK-CO-15 (27), expresses endogenously 75-kD NGF receptor on the apical membrane (Le Bivic, A., unpublished results). However, analysis of the sorting of a pulse of newly synthesized WT hNGFR by the addition of antibody to the apical or the basolateral medium during the

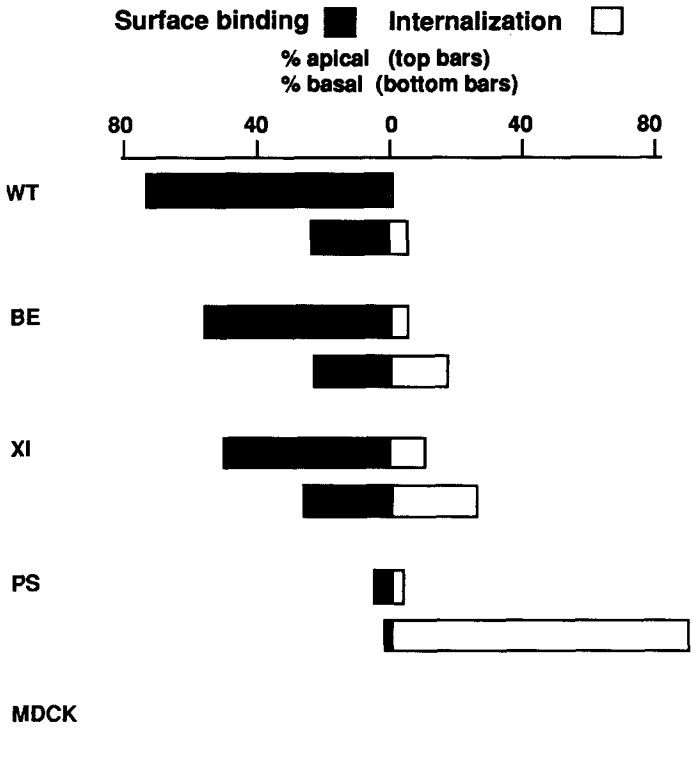

	cpm	
	Surface binding	Internalization
WT	6579	81
	2075	455
BE	1401	145
	603	365
XI	141	28
	99	95
PS	42	22
	4	589
MDCK	18	0
	20	0

Figure 9. NGF binding and internalization in transfected MDCK cells. Confluent monolayers on polycarbonate filters were incubated 1 h at 37°C with ^{125}I-NGF with or without an excess of cold NGF (1,000×), from the apical or the basolateral side, and then washed at 4°C with PBS-CaMg. Filters were then acid washed as described (see Materials and Methods) to determine the surface bound ^{125}I-NGF and the radioactivity still associated to the filter after acid wash was counted as internalized NGF. Results are corrected for nonspecific binding in the presence of excess cold NGF. (*Left*) Results are expressed as percent of total cell associated radioactivity. For each construct, top bars represent binding and internalization from the apical side and bottom bars idem from the basolateral side. 100% of cell associated NGF is the sum of top and bottom bars (binding plus internalization). (*Right*) the corresponding surface binding and internalization cpm are shown for each construct; top numbers correspond to apical and bottom numbers to the basolateral side. Control untransfected MDCK cells showed only background binding. Standard deviation was <15% and experiments were done several times in duplicate or triplicate. Whereas bound NGF is mainly at the cell surface in cells expressing WT hNGFR, it is mainly intracellular in cells expressing the PS mutant.

chase detected the same fraction of apical hNGFR (80%) as in steady state, suggesting that transcytosis probably plays a negligible role in determining its steady state distribution. This is in agreement with the observation that the hNGFR expressed in MDCK cells is of the low affinity type and is poorly endocytosed.

Role of hNGFR Domains in Sorting

Having established that WT hNGFR is apically sorted, we investigated the domain localization of the putative sorting signals. The extracellular domain of hNGFR contains four 40 amino acid repeats with six cysteine residues at conserved positions followed by a serine/threonine-rich region (the site of attachment of several *O*-linked sugars), a single transmembrane domain, and a 155 amino acid cytoplasmic domain containing two tyrosines and a serine phosphorylation site (21). Deletion of the region containing attachment sites for *O*-linked sugars (BE construct) had no effect on the apical expression of the mutant hNGFR or on its stability suggesting that *O*-linked carbohydrates are not involved in the apical sorting of hNGFR via clustering with membrane sphingolipids (63).

We then examined the role of the cytoplasmic domain in targeting of hNGFR. Deletion of 150 out of 155 amino acids of the cytoplasmic tail (XI mutant) did not alter the polarized expression of hNGFR (still ~80% apical), which restricts the localization of the putative apical signal to the transmembrane and/or ecto domains. Several plasma membrane proteins with the apical surface as the final destination appear to possess apical targeting information in the ectodomain (39, 40, 42). Moreover, GPI-anchored proteins which lack a cytoplasmic domain are preferentially expressed on the apical membrane of epithelial cells, with apical targeting information contained in the GPI, in the protein ectodomain, or in both (33, 34, 68).

Basolateral Localization of A Mutant hNGFR with An Internal Deletion in the Cytoplasmic Tail

A surprising result was obtained when we analyzed the effect of a 57 amino acid deletion within the cytoplasmic domain of the hNGFR. This mutant receptor (PS mutant) was expressed almost exclusively on the basolateral membrane (95%). The reversed polarity of this mutant receptor was shown to be the result of altered intracellular sorting at the TGN by a continuous antibody targeting assay. An ^{125}I-NGF binding and internalization assay detected very little intracellular accumulation of NGF from the apical side, confirming that PS hNGFR does not transit through the apical membrane. The binding assay unveiled another surprising result: a 100–200-fold increase in the endocytosis of ligand by the mutant receptor as compared with WT hNGFR. Analysis of the internalization of NGF from both apical and basolateral surfaces indicated that this increased endocytic capacity was an intrinsic property of the receptor, since the basolaterally internalized NGF was at least 100 times greater than the basolateral surface binding for PS hNGFR but smaller than the basolateral surface binding for WT, BE, and XI receptors. However, part of the increased endocytic ability of NGF

by PS hNGFR may be attributed to its preferential basolateral localization, since specific internalization, normalized by the amount of receptor, was ~10–15 times higher from the basolateral side for all forms of hNGFR. Similarly, endogenous MDCK LDL receptor, which is expressed with slight preference for the basolateral surface (~2/3 of total surface binding) endocytoses and degrades LDL 6-10 times more efficiently from the basolateral side (29). Perhaps, this reflects a higher nonspecific internalization rate of the basolateral plasma membrane. Although rates of internalization of fluid markers are similar for both membranes of MDCK cells, the rates of bulk internalization of both membranes have not been measured (4, 67).

A possible interpretation of our results is that the PS mutant of NGFR expresses a new basolateral targeting signal in the cytoplasmic domain that is dominant over apical targeting information in the ecto/transmembrane domains. This basolateral "signal" modifies the sorting of the receptor intracellularly, most likely at the level of the TGN, so that the mutant receptor is targeted vectorially to the basolateral surface. Alternatively, the deletion in the cytoplasmic domain might introduce a conformational change in the hNGFR that prevents recognition of the apical targeting signal by the apical targeting machinery. Our results do not allow us to discriminate fully between these two possibilities. However, since deletion of almost the entire cytoplasmic domain does not alter the apical localization the first possibility appears as the most likely one.

Recent results are consistent with the presence of basolateral targeting information in the cytoplasmic domain of certain plasma membrane proteins. Such a role for the cytoplasmic domain was shown first for the pIgR. A tail-minus pIgR is transported directly to the apical membrane, instead of via the transcytotic route (42). The information for basolateral targeting is contained within 17 juxtamembrane cytoplasmic amino acids and can be transferred to other proteins (10). A result similar to the one described here for hNGFR was recently reported for the FcRII of macrophages and leukocytes. Two natural isoforms that differ only by an in frame insertion of 47 amino acids in their cytoplasmic domains, have an opposite polarity after transfection in epithelial cells (20). This work did not determine, however, whether the altered (basolateral) distribution of the FcRII with the long cytoplasmic tail was because of altered intracellular sorting and vectorial basolateral targeting or to newly acquired transcytotic ability. Very recent results (21a) indicate that the first possibility (i.e., basolateral sorting) is the correct one. Independent evidence for a role of cytoplasmic domains in basolateral targeting is suggested by the experiments of Brown et al. (6). These workers showed that attachment of placental alkaline phosphatase to transmembrane and cytoplasmic regions of VSV G protein resulted in the basolateral localization of the fusion protein (6). Whether the transmembrane or the cytoplasmic domains of VSV G carry the sorting information and whether vectorial targeting accounts for basolateral location is not known.

Increased Endocytosis of PS hNGFR

Another important new property of the PS mutant of the hNGFR is its highly increased ability for endocytosis of NGF. As was pointed out, the deletion brings Tyr 308 into a more favorable environment to be recognized as an endocytic signal (Fig. 4 *B*). It is unlikely that increased endocytosis of PS hNGFR be a result of nonspecific effects such as aggregation, since no unusual oligomerization is detected by crosslinking experiments in fibroblasts expressing this mutated hNGFR (19). Several groups have characterized the role of tyrosine and neighboring residues in endocytosis (11, 23, 24, 38). Roth and his co-workers have shown that addition of a tyrosine residue (tyr 543) to the short cytoplasmic domain of influenza HA (Fig. 4 *B*) promotes efficient endocytosis of this normally poorly internalized molecule (24). Recent work indicates that an environment of polar or charged amino acids in the vicinity of tyrosine promotes endocytosis even further (11, 23, 24, 38). In the PS hNGFR mutant, tyrosine 308, located 64 amino acids away from the membrane in the wild type receptor, is located seven amino acids from the lipid bilayer in the immediate neighborhood of several polar or charged residues (Fig. 4 *B*). It is tempting to speculate that this is an important factor in the acquisition of endocytic ability by PS hNGFR; however, direct proof of this point will require removal of Tyr 308 by site-directed mutagenesis. Because the most distal tyrosine residue (Tyr 340) is surrounded completely by hydrophobic amino acids, it is unlikely that it plays a role in endocytosis.

Endocytic ability and basolateral targeting have been correlated in some instances. Influenza HA with a new tyrosine residue in its short (10 amino acids) cytoplasmic tail is targeted to the basolateral membrane in transfected MDCK cells (6a). Furthermore, whereas WT LDL receptor is targeted to the basolateral membrane of transfected MDCK cells, an LDL receptor mutant defective in endocytosis, a result of deletion of the cytoplasmic domain, is delivered to the apical surface (21a, ref. cited). The basolateral FcRII isoform has also increased affinity for coated pits whereas the apical isoform is excluded from coated pits (20). However, exceptions to this rule also exist. In transgenic mice, the LDL receptor is expressed apically in kidney cells, where it is concentrated in coated pits, but is localized basolaterally in liver and intestine cells, where it is excluded from coated pits (44). A pIgR mutant with a deletion of all but the 17 proximal tail amino acids is still basolateral but is not endocytosed whereas another mutant lacking the 14 proximal tail amino acids is apical (10). Thus, in some cases (FcR, influenza HA, hNGFR, and LDL receptor in MDCK cells) endocytic ability correlates with basolateral targeting whereas in other cases (PolyIgR, LDL receptor in transgenic mice) these two properties can be dissociated. Thus, basolateral targeting signals may be similar but not identical to endocytic signals.

The correlation between endocytic ability and basolateral targeting (where observed) would suggest a possible sorting role for TGN adaptor proteins. Adaptor proteins have been classified into two classes, HA1, found in Golgi-coated pits and HA2, found in plasma membrane–coated pits (1, 47, 48). Both HA1 and HA2 bind to the cytoplasmic domain of the calcium independent mannose-6-phosphate receptor but a receptor mutated in its tail tyrosine still interacts with HA1 but not with HA2, which demonstrates that these two adaptors recognize different features in the tail (13). It must be noted too that the CI-M6PR is detected only at the basolateral surface of MDCK cells (45). It may be speculated that an adaptor at the Golgi level, possibly HA1, recognizes a basolateral signal in the tail of some basolateral proteins re-

sulting in their recruiting into basolaterally targeted vesicles or preventing their incorporation into apical carrier vesicles.

It has been proposed that in epithelial cells only the apical pathway is signal mediated whereas the basolateral pathway is default (58). This suggestion was made on the basis of two lines of evidence. First, the basolateral membrane is thought to be equivalent to the plasma membrane of nonpolarized cells and there is some evidence that transport from the TGN to the plasma membrane occurs by default in nonpolarized cells (22). Second, apical proteins frequently leak into the basolateral route whereas the opposite (basolateral proteins significantly leaking into the apical pathway) has not been observed yet. The results presented in this report and work from other laboratories (20, 42, 43) suggest that, at least for some basolateral proteins, there may be a signal involved in their targeting to the basolateral membrane and therefore transport to the basolateral membrane would not be a default mechanism.

We thank Ms. Lori van Houten for photographic work.

This work was supported by grants from the National Institutes of Health (GM 34107 to E. Rodriguez-Boulan and NS 21072 to M. Chao), New York Heart Association, and American Cancer Society. A. Le Bivic was supported by UA179 from Centre National de la Recherche Scientifique and A. Patzak by a Charles H. Revson fellowship.

Received for publication 14 March 1991 and in revised form 16 July 1991.

References

1. Ahle, S., A. Mann, U. Eichelsbacher, and E. Ungewickell. 1988. Structural relationships between clathrin assembly proteins from the golgi and the plasma membrane. *EMBO (Eur. Mol. Biol. Organ.) J.* 4:919–929.
2. Bartles, J. R., H. M. Feracci, B. Stieger, and A. L. Hubbard. 1987. Biogenesis of the rat hepatocyte plasma membrane in vivo: comparison of the pathways taken by apical and basolateral proteins using subcellular fractionation. *J. Cell Biol.* 105:1241–1251.
3. Bernd, P. 1986. Characterization of nerve growth factor binding to cultured neural crest cells: evidence of an early developmental form of the NGF receptor. *Dev. Biol.* 115:415–424.
4. Bomsel, M., K. Prydz, R. G. Parton, J. Gruenberg, and K. Simons. 1989. Endocytosis in filter grown Madin-Darby Canine kidney cells. *J. Cell Biol.* 109:3243–3258.
5. Breitfeld, P. P., J. E. Casanova, N. E. Simister, S. A. Ross, W. C. Mckinnon, and K. E. Mostov. 1989. Sorting Signals. *Curr. Op. Cell Biol.* 1:617–623.

6a. Brewer, C. B., and M. G. Roth. 1991. A single amino acid change in the cytoplasmic domain alters the polarized delivery of influenza virus hemagglutinin. *J. Cell Biol.* 114:413–421.

6. Brown, D. A., B. Crise, and J. K. Rose. 1989. Mechanism of membrane anchoring affects polarized expression of two proteins in MDCK cells. *Science (Wash. DC).* 245:1499–1501.
7. Caplan, M., B. Forbush, G. Palade, and J. Jamieson. 1990. Biosynthesis of the Na,K-ATPase in MDCK cells. *J. Biol. Chem.* 6:3528–3534.
8. Caplan, M. J., H. C. Anderson, G. E. Palade, and J. D. Jamieson. 1986. Intracellular sorting and polarized cell surface delivery of (Na^+,K^+) ATPase, an endogenous component of MDCK cell basolateral plasma membranes. *Cell.* 46:623–631.
9. Caplan, M. J., and K. S. Matlin. 1989. The sorting of membrane and secretory proteins in polarized epithelial cells. In Functional Epithelial Cells in Culture. K. S. Matlin and J. D. Valentich, editors. Alan R. Liss, Inc., New York. 71–130.
10. Casanova, J. E., G. Apodaca, and K. E. Mostov. 1991. An autonomous signal for basolateral sorting in the cytoplasmic domain of the polymeric immunoglobulin receptor. *Cell.* 66:65–75.
11. Collawn, J. F., M. Stangel, L. A. Kuhn, V. Esekogwu, S. Jing, I. S. Trowbridge, and J. A. Tainer. 1990. Transferrin receptor internalization sequence YXRF implicates a tight turn as a structural recognition motif for endocytosis. *Cell.* 63:1061–1072.
12. Compton, T., I. E. Ivanov, T. Gottlieb, M. Rindler, M. Adesnik, and D. D. Sabatini. 1989. A sorting signal for the basolateral delivery of the vesicular stomatitis virus (VSV) G protein lies in its luminal domain: Analysis of the targeting of VSV G-influenza hemagglutinin chimeras. *Proc. Natl. Acad. Sci. USA.* 86:4112–4116.
13. Glickman, J. N., E. Conibear, and B. M. F. Pearse. 1989. Specificity of binding adaptors to signals on the mannose-6-phosphate/insulin-like growth factor II receptor. *EMBO (Eur. Mol. Biol. Organ.) J.* 8:1041–1047.
14. Goding, J. W. 1976. The chromic chloride method of coupling antigens to erythrocytes: definitions of some important parameters. *J. Immunol. Meth.* 10:61–66.
15. Graham, F., and A. Van der Eb. 1973. A new technique for the assay of infectivity of human adenovirus 5 DNA. *Virology.* 52:456–467.
16. Greenwood, F. C., W. M. Hunter, and S. J. Glover. 1963. The preparation of 125I-labelled human growth hormone of high specific radioactivity. *Biochem. J.* 89:114–123.
17. Griffiths, G., and K. Simons. 1986. The trans Golgi network: sorting at the exit site of the Golgi complex. *Science (Wash. DC).* 234:438–443.
18. Griffiths, G., K. Simons, G. Warren, and K. T. Tokuyasu. 1983. Immunoelectron microscopy using thin, frozen sections: application to studies of the intracellular transport of Semliki Forest virus spike glycoproteins. *Methods Enzymol.* 96:466–485.
19. Hempstead, B. L., N. Patil, B. Thiel, and M. V. Chao. 1990. Deletion of the cytoplasmic sequences of the nerve growth factor receptor leads to loss of high affinity ligand binding. *J. Biol. Chem.* 265:9595–9598.
20. Hunziker, W., and I. Mellman. 1989. Expression of macrophage-lymphocyte Fc Receptors in Madin-Darby Canine Kidney cells: polarity and transcytosis differ for isoforms with or without coated pit localization domains. *J. Cell Biol.* 109:3291–3302.

21a. Hunziker, W., C. Harter, K. Matter, and I. Mellman. 1991. Basal lateral sorting in MDCK cells requires a distinct cytoplasmic domain determinant. *Cell.* 66:907–920.

21. Johnson, D., A. Lanahan, C. R. Buck, A. Sehgal, C. Morgan, E. Mercer, M. Bothwell, and M. Chao. 1986. Expression and structure of the human NGF receptor. *Cell.* 47:545–554.
22. Karrenbauer, A., D. Jeckel, W. Just, R. Birk, R. R. Schmidt, J. E. Rothman, and F. T. Wieland. 1990. The rate of the bulk flow from the golgi to the plasma membrane. *Cell.* 63:259–267.
23. Ktistakis, N. T., D. Thomas, and M. G. Roth. 1990. Characteristics of the tyrosine recognition signal for internalization of transmembrane surface glycoproteins. *J. Cell Biol.* 111:1393–1407.
24. Lazarovits, J., and M. Roth. 1988. A single amino acid change in the cytoplasmic domain allows the influenza virus hemagglutinin to be endocytosed through coated pits. *Cell.* 53:743–752.
25. Le Bivic, A., A. Quaroni, B. Nichols, and E. Rodriguez-Boulan. 1990. Biogenetic pathways of plasma membrane proteins in Caco-2, a human intestinal epithelial cell line. *J. Cell Biol.* 111:1351–1361.
26. Deleted in proof.
27. Le Bivic, A., F. X. Real, and E. Rodriguez-Boulan. 1989. Vectorial targeting of apical and basolateral plasma membrane proteins in a human adenocarcinoma epithelial cell line. *Proc. Natl. Acad. Sci. USA.* 86:9313–9317.
28. Le Bivic, A., Y. Sambuy, K. Mostov, and E. Rodriguez-Boulan. 1990. Vectorial targeting of an endogenous apical membrane sialoglycoprotein and uvomorulin in MDCK cells. *J. Cell Biol.* 110:1533–1539.
29. Li, C., S. Stifani, W. J. Schneider, and M. J. Poznansky. 1991. Low density lipoprotein receptors on epithelial cell (Madin-Darby canine kidney) monolayers. Asymmetric distribution correlates with functional difference. *J. Biol. Chem.* 266:9263–9270.
30. Lisanti, M., I. P. Caras, M. A. Davitz, and E. Rodriguez-Boulan. 1989. A glycolipid membrane anchor acts as an apical targeting signal in polarized epithelial cells. *J. Cell Biol.* 109:2145–2156.
31. Lisanti, M., A. Le Bivic, M. Sargiacomo, and E. Rodriguez-Boulan. 1989. Steady state distribution and biogenesis of endogenous MDCK glycoproteins: evidence for intracellular sorting and polarized cell surface delivery. *J. Cell Biol.* 109:2117–2128.
32. Lisanti, M., and E. Rodriguez-Boulan. 1990. Glycolipid membrane anchoring provides clues to the mechanism of protein sorting in polarized epithelial cells. *TIBS (Trends Biochem. Sci.)* 15:113–118.
33. Lisanti, M., M. Sargiacomo, L. Graeve, A. Saltiel, and E. Rodriguez-Boulan. 1988. Polarized apical distribution of glycosyl phosphatidylinositol anchored proteins in a renal epithelial line. *Proc. Natl. Acad. Sci. USA.* 85:9557–9561.
34. Lisanti, M. P., A. Le Bivic, A. Saltiel, and E. Rodriguez-Boulan. 1990. Preferred apical distribution of glycosyl-phosphatidylinositol (GPI) anchored proteins: a highly conserved feature of the polarized epithelial cell phenotype. *J. Memb. Biol.* 113:155–167.
35. Massey, D., H. Feracci, J. P. Gorvel, A. Rigal, J. M. Soulie, and S. Maroux. 1987. Evidence for the transit of aminopeptidase N through the basolateral membrane before it reaches the brush border of enterocytes. *J. Membr. Biol.* 96:19–25.
36. Matlin, K. S., and K. Simons. 1984. Sorting of an apical plasma membrane glycoprotein occurs before it reaches the cell surface in cultured epithelial cells. *J. Cell Biol.* 99:2131–2139.
37. Matter, K., M. Brauchbar, K. Bucher, and H. P. Hauri. 1990. Sorting of endogenous plasma membrane proteins occurs from two sites in cultured human intestinal epithelial cells (Caco-2). *Cell.* 60:429–437.
38. McGraw, T. E., and F. R. Maxfield. 1990. Human transferrin receptor internalization is partially dependent upon an aromatic amino acid on the cytoplasmic domain. *Cell Regul.* 1:369–377.
39. McQueen, N. L., D. P. Nayak, E. B. Stephens, and R. W. Compans. 1986.

Polarized expression of a chimeric protein in which the transmembrane and cytoplasmic domains of the influenza virus hemagglutinin have been replaced by those of the vesicular stomatitis virus G protein. *Proc. Natl. Acad. Sci. USA.* 83:9318-9322.
40. McQueen, N. L., D. P. Nayak, E. B. Stephens, and R. W. Compans. 1987. Basolateral expression of a chimeric protein in which the transmembrane and cytoplasmic domains of vesicular stomatitis virus G protein have been replaced by those of the influenza virus hemagglutinin. *J. Biol. Chem.* 262:16233-16240.
41. Misek, D. E., E. Bard, and E. Rodriguez-Boulan. 1984. Biogenesis of epithelial cell polarity: intracellular sorting and vectorial exocytosis of an apical plasma membrane glycoprotein. *Cell.* 39:537-546.
42. Mostov, K. E., P. Breitfeld, and J. M. Harris. 1987. An anchor-minus form of the polymeric immunoglobulin receptor is secreted predominantly apically in Madin-Darby canine kidney cells. *J. Cell Biol.* 105:2031-2036.
43. Mostov, K. E., A. B. Kops, and D. L. Deitcher. 1986. Deletion of the cytoplasmic domain of the polymeric immunoglobulin receptor prevents basolateral localization and endocytosis. *Cell.* 47:359-364.
44. Pathak, R. K., M. Yokode, R. E. Hammer, S. L. Hofmann, M. S. Brown, J. L. Goldstein, and R. G. W. Anderson. 1990. Tissue-specific sorting of the human LDL receptor in polarized epithelia of transgenic mice. *J. Cell Biol.* 111:347-359.
45. Prydz, K., A. W. Brandli, M. Bomsel, and K. Simons. 1990. Surface distribution of the mannose 6-phosphate receptors in epithelial Madin-Darby canine kidney cells. *J. Biol. Chem.* 265:12629-12635.
46. Radeke, M. J., T. P. Misko, C. Hsu, L. A. Herzenberg, and E. M. Shooter. 1987. Gene transfer and molecular cloning of the rat nerve growth factor receptor. *Nature (Lond.).* 325:593-597.
47. Robinson, M. S. 1987. 100K coated vesicle proteins: molecular heterogeneity and intracellular distribution studied with monoclonal antibodies. *J. Cell Biol.* 104:887-895.
48. Robinson, M. S., and B. M. F. Pearse. 1986. Immunofluorescence localization of 100K coated vesicle proteins. *J. Cell Biol.* 102:48-54.
49. Rodriguez-Boulan, E. 1983. Polarized assembly of enveloped viruses from cultured epithelial cells. *Methods Enzymol.* 98:486-501.
50. Rodriguez-Boulan, E., and W. J. Nelson. 1989. Morphogenesis of the Polarized Epithelial Cell Phenotype. *Science (Wash. DC).* 245:718-725.
51. Roman, L. M., and H. Garoff. 1986. Alteration of the cytoplasmic domain of the membrane-spanning glycoprotein p62 of Semliki Forest virus does not affect its polar distribution in established lines of Madin-Darby canine kidney cells. *J. Cell Biol.* 103:2607-2618.
52. Rose, J. K., and R. W. Doms. 1988. Regulation of protein export from the endoplasmic reticulum. *Annu. Rev. Cell Biol.* 4:257-288.
53. Ross, A. H., P. Grob, M. Bothwell, D. E. Elder, C. S. Ernst, N. Marano, B. F. D. Ghrist, C. C. Slemp, M. Herlyn, B. Atkinson, and H. Koprowski. 1984. Characterization of nerve growth factor receptor in neural crest tumors using monoclonal antibodies. *Proc. Natl. Acad. Sci. USA.* 81:6681-6685.
54. Roth, M. G., D. Gundersen, N. Patil, and E. Rodriguez-Boulan. 1987. The large external domain is sufficient for the correct sorting of secreted or chimeric influenza virus hemagglutinins in polarized monkey kidney cells. *J. Cell Biol.* 104:769-782.
55. Sambuy, Y., and E. Rodriguez-Boulan. 1988. Isolation and characterization of the apical surface of polarized Madin-Darby canine kidney epithelial cells. *Proc. Natl. Acad. Sci. USA.* 85:1529-1533.
56. Sargiacomo, M., M. Lisanti, L. Graeve, A. Le Bivic, and E. Rodriguez-Boulan. 1989. Integral and peripheral protein compositions of the apical and basolateral membrane domains in MDCK cells. *J. Memb. Biol.* 107:277-286.
57. Simonoski, K., P. Gonnella, J. Bernanke, L. Owen, M. Neutra, and R. Murphy. 1986. Uptake and transepithelial transport of NGF in suckling rat ileum. *J. Cell Biol.* 103:1979-1990.
58. Simons, K., and A. Wandinger-Ness. 1990. Polarized sorting in epithelia. *Cell.* 62:207-210.
59. Slot, G. E. R., and H. J. Geuze. 1985. A new method for preparing gold probes for multiple labelling cytochemistry. *Eur. J. Cell Biol.* 38:87-93.
60. Stephens, E. B., and R. W. Compans. 1988. Assembly of animal viruses at cellular membranes. *Ann. Rev. Microbiol.* 42:489-516.
61. Tarentino, A. L., R. B. Trimble, and T. H. Plummer. 1989. Enzymatic approaches for studying the structure, synthesis, and processing of glycoproteins. *Methods Cell Biology.* 32:111-139.
62. Tokuyasu, K. T. 1973. A technique for ultracryotomy of cell suspensions and tissues. *J. Cell Biol.* 57:551-565.
63. van Meer, G. 1989. Lipid traffic in animal cells. *Annu. Rev. Cell Biol.* 5:247-275.
64. van Meer, G., and K. Simons. 1988. Lipid polarity and sorting in epithelial cells. *J. Cell Biochem.* 36:51-58.
65. van Meer, G., E. H. Stelzer, Resandt. R. W. Wijnaendts van, and K. Simons. 1987. Sorting of sphingolipids in epithelial (Madin-Darby canine kidney) cells. *J. Cell Biol.* 105:1623-1635.
66. Vega Salas, D. E., P. J. Salas, D. Gundersen, and E. Rodriguez-Boulan. 1987. Formation of the apical pole of epithelial (Madin-Darby canine kidney) cells: polarity of an apical protein is independent of tight junctions while segregation of a basolateral marker requires cell-cell interactions. *J. Cell Biol.* 104:905-916.
67. von Bonsdorff, C. H., S. D. Fuller, and K. Simons. 1985. Apical and basolateral endocytosis in Madin-Darby canine kidney (MDCK) cells grown on nitrocellulose filters. *EMBO (Eur. Mol. Biol. Organ.) J.* 4:2781-2792.
68. Wilson, J. M., N. Fasel, and J.-P. Kraehenbuhl. 1990. Polarity of endogenous and exogenous glycosyl-phosphatidylinositol-anchored membrane proteins in Madine Darby canine kidney cells. *J. Cell Sci.* 96:143-149.